

Factors Affecting Special Core Analysis Resistivity Parameters

Hassan M. Sbiga,

Libyan Petroleum Institute (L.P.I)

Tripoli-Libya

hasanespiga@yahoo.com hasanespiga@gmail.com

Saber Elmabrouk

Petroleum Engineering Department

Tripoli University

Tripoli-Libya

saber_elmabrouk@yahoo.com

Walid Mohamed Mahmud

Petroleum Engineering Department

Tripoli-University

Tripoli-Libya

walidt@hotmail.com

Abstract

Laboratory measurements methods were undertaken on core samples selected from three different fields (A, B, and C) from the Nubian sandstone formation in Libya. These measurements were conducted in order to determine factors that may affect resistivity parameters, and to investigate the effect of rock heterogeneity and wettability on these parameters. This included determining the saturation exponent (n) in the laboratory at two stages. The first stage was before wettability measurements were conducted on the samples, and the second stage was after the wettability measurements in order to find any effect on the saturation exponent. Changes were observed in formation resistivity factor and cementation exponent due to ambient conditions and changes of overburden pressure. Variations were also observed in the saturation exponent (n) and water saturation (S_w) before and after wettability measurements. Samples that have oil-wet tendency have higher irreducible brine saturation and higher Archie saturation exponent values than samples having a uniform water-wet surface. The experimental results indicate that there is a good relation between resistivity and pore type depending on the pore size. When oil begins to penetrate micro-pore systems in measurements of resistivity index versus brine saturation (after wettability measurement), a significant change in slope of the resistivity index relationship occurs.

Keywords

Ambient Condition, Cementation, Resistivity, Saturation, Wettability.

Introduction

This work was conducted to investigate the effect of rock heterogeneity and wettability on resistivity parameters of sandstone reservoir rocks, Nubian sandstone, and quantify experimentally pore and porosity types (macro- and micro-porosity), which have an affect on the electrical properties, by integrating capillary pressure curves with other routine and special core analysis. These experiments were made for the first time to obtain a relationship between pore size distribution and saturation exponent n. The interpretation of logging data is based on Archie's law. Electrical logging is the most widely used method of identifying hydrocarbon intervals in wellbore. Standard method of relating oil saturation in clay free reservoirs to electrical resistivity is based on Archie saturation equation Archie (1942):

$$RI = \frac{R_t}{R_o} = S_w^{-n} \quad (1)$$

Where the resistivity index, RI, is equal to the ratio of the resistivity of the sample (R_t) at brine saturation (S_w) over the resistivity of the sample at one hundred percent brine saturation (R_o). The resistivity index is related to the saturation of the sample and the saturation exponent (n). The saturation exponent must be determined by experimental core analysis. The standard technique for determining the saturation exponent involves measurements in cleaned cores, usually with air as the non-wetting phase and brine phases. This air/brine system is only representative of the drainage conditions in strongly water-wet cases. When oil is displaced by water, for instance during water flooding, different distributions of fluids may prevail at the pore scale due to hysteresis effects controlled by pore geometries, initial saturation and wettability distribution at the pore scale. Wyble (1958) found a systematic decrease in the rock conductivity and an increase in formation factor as the overburden pressure increased over the range of 0 to 3500 psi using core samples. In the study carried out by Wyble (1958), an increase in formation factor of up to 6.6 percent of original value measured at zero overburden pressure. Cementation exponent of one of the samples studied was increased from 1.87 to 2.04 as a result of increasing the pressure up to 5000 psi. Porosity of sedimentary rocks can be classified according to their pore size distribution as macro- and micro-porosity. Vuggy and fracture porosities are characteristics of macro-porosity because large pore geometries are associated with vugs and fractures. Pore system associated with macro-porosity has an average pore diameter greater than 1/16 mm, Pittman (1971) where most of the hydrocarbon volume accumulates. Permeability is strongly dependent on the amount of macro-porosity. Micro-porosity is associated with pores whose diameter is less than 1/16 mm, Pittman (1971). Micro-porous system is characterized by a high capillary pressure, which tends to retain high amount of irreducible water resulting in high formation electrical conductivity (low resistivity).

Wettability plays a major role in controlling the distribution of fluids within the pore space inside a rock. Keller (1953), presented evidence that saturation exponent could be substantially different from 2.0. He found that Archie's saturation exponent (n) varies from 1.5 to 11.7 for the same rock, depending on how cores were treated. For the same water saturation, resistivity of an oil reservoir can vary thousand times for different wetting conditions. The wettability of sandstone cores was altered from water wet to oil wet conditions by using various chemical treatments. Keller (1953) concluded that the wettability played a great role in the fluid distribution within the rock space. By changing the relative position of the conducting fluid with respect to the rock surface, the electric behavior of fluid filled sandstone would also change. Measurements of capillary pressure curves as means of determining pore size distribution was first suggested by Washburn (1921). This principle was fairly accepted and the majority of the pore size distribution measurements have been determined by the mercury injection procedure.

Methodology

Core data of porosity and permeability of Nubian sandstone formation (6 wells, A-01, A-02, A-03, B-01, C-01, and C-02) are presented in Table 1. Figure 1 illustrates the location of the studied fields. Core samples were selected to study the petrophysical parameters and their effect on resistivity. One and a half inch diameter core plugs were cut from full diameter core in the horizontal direction using a diamond core bit with water as the bit coolant and lubricant. The samples were extracted of hydrocarbons using toluene, leached of salt using methanol, and oven dried at 80 °C for a period of 48 to 72 hours, and then left to cool to room temperature before conventional core analysis commenced.

The clean, dry samples were subjected to various analyses to determine porosity, permeability and grain density values where possible. The core analysis laboratory of the Libyan Petroleum Institute uses a twin cell helium expansion gas porosimeter for the plug sample grain volume measurement. The porosimeter operates using the principle of Boyle's Law. A sealed reference chamber in the instrument is filled with helium gas at ambient temperature to a pressure of 100 psi. A sample is placed in another sealed chamber, connected to the reference chamber by a two-way valve. This valve when opened allows the gas in the reference chamber to expand into the combined volume of the two chambers. From Boyle's Law, the volume of the sample chamber can be calculated when the volume of the reference chamber, the initial pressure and the final pressure are known. The instrument must be calibrated beforehand. This is done by running a series of stainless steel blanks of known volumes, to build up a graph of blank volume versus the inverse of the final pressure. The resulting calibration graph has to be entered into a computer program which performs a linear regression, producing an equation relating the grain volume of any sample run to the final pressure reading. The porosity and the grain density are then calculated by determining the bulk volume, and the weight of the sample. The porosity of the sample calculated as follows:

$$\phi = \frac{V_P}{V_b} = \frac{V_P}{V_P + V_g} \quad (2)$$

Where:

- ϕ = Fractional Porosity
- V_P = Pore volume, C.C
- V_b = Bulk volume, C.C
- V_g = Grain volume, C.C

For permeability measurement, a clean, dry sample is placed in the Hassler-type core holder and an overburden pressure of 200 psi (industry standard practice to sample) is applied to the cell, compressing the rubber sleeve around the sample. Nitrogen gas pressure is applied to one end face of the sample, whilst the other end face is open to atmospheric pressure, causing the gas to flow through the sample. The flow of gas is measured at the low pressure (downstream) end face of the sample. The flow rate is measured by passing the gas through one of three laminar flow orifices and the differential pressure developed across the orifice is also measured. The transducers and flow orifices are calibrated using a dead weight tester and soap film meter at least once every three months, or when any component is altered or replaced. The length of the sample, upstream and downstream pressures, flow rate, viscosity of nitrogen, barometric pressure and temperature are entered into Darcy's equation for gas permeability, and the permeability of the sample calculated as follows:

$$K_g = \frac{2000 \times P_a \times Q \times \mu_g \times L}{(P_1^2 - P_2^2) \times A} \quad (3)$$

Where:

- K_g = Gas permeability (mD)
- P_a = Barometric pressure (atm)
- P_1 = Upstream pressure (atm)
- P_2 = Downstream pressure (atm)
- Q = Gas flow rate (cc/sec.)
- μ_g = Gas viscosity (cp)
- L = Sample length (cm)
- A = Cross-sectional area (sq.cm)

The samples belong to Nubian sandstone from three oil fields as shown in Table 1, Sirt basin were selected to perform formation resistivity factor measurements.

Table 1. Porosity and permeability values of the studied wells.

Samples#	Well Name	Porosity (%)	Permeability (mD)
03	A1-Libya	10.39	337.5
10	A1-Libya	9.01	34.11
15	A3-Libya	12.17	12.55
18	B1-Libya	14.59	1146
24	A3-Libya	8.01	9.910
29	C2-Libya	17.38	69.86
41	C1-Libya	15.34	660.4
42	A3-Libya	11.71	4.901
47	C2-Libya	17.91	279.7
53	A1-Libya	11.16	297.7
83	A2-Libya	9.56	27.73
123	A2-Libya	12.76	118.1

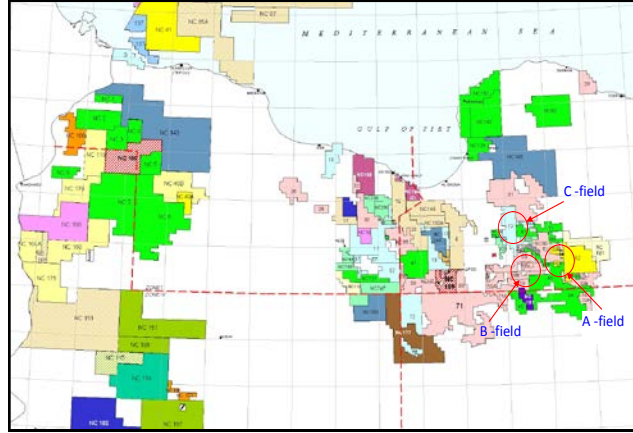


Fig.1. Location oil fields proposed in this study.

The formation resistivity factor was measured for the twelve samples. The clean and dry samples were loaded in a stainless steel saturator and evacuated for 12 hours. A solution of 135,000 ppm sodium chloride was introduced at the end of this period, followed by pressurizing the system at 2000 psi for 12 hours to assist penetration. The brine saturated plugs were placed in turn between electrodes at 1 KHz frequency and their electrical resistance were measured on consecutive days until ionic equilibrium was achieved between the fluid and rock sample. Formation resistivity factor measurements were made on 100 percent brine saturated core samples at ambient conditions and the elevated reservoir overburden pressure. The sample resistance was measured and converted to resistivity using the sample cross-sectional area and length. Formation resistivity factor is calculated as the ratio of the sample resistivity to the resistivity of the water saturating it. The formation resistivity factors of a group of samples are plotted versus their porosities on log-log graph paper. The slope of the best fit line is the value of the cementation factor, “m”, and the intercept is the value of “a”.

$$F.F = \frac{a}{\phi^m} \quad (4)$$

The previous samples were used for the formation resistivity factor measurements at room conditions and scheduled for formation factor testing at overburden pressure (1000- 5000 psi) and formation resistivity index test. The wettability measurements were conducted on the samples using Amott method then some samples were selected to perform capillary pressure measurements. Mercury injection offers an alternative system for the study of capillary pressure. Mercury injection method entails injecting mercury into a clean dry sample and monitoring the injection pressure and the amount of mercury injected into the rock sample. Pore size distribution can be calculated from mercury injection capillary pressure data; however, a broad range of pore size and type is covered by mercury injection capillary pressure. The pore throat radius is calculated as:

$$r_p = \frac{2\sigma \cos \theta}{P_c} \quad (5)$$

Where

- r_p Pore throat radius, cm
- σ Interfacial tension, dynes/cm
- θ Contact angle, degree
- P_c Capillary pressure, dyne/cm²

In an air-mercury system where $\sigma= 480$ dyne/cm, $\theta=140^\circ$ and pressure in psi, the pore entry radius in microns can be determined as follows:

$$r_p (\text{micron}) = \frac{106}{P_c (\text{psi})} \quad (6)$$

Results

Twelve sandstone core samples were selected from six wells and three different oil fields. Porosities of samples varied from 8.01 to 17.91% and permeability ranged from 4.90mD to 1146 mD as presented in Table 1, while the other properties such as formation resistivity factor, porosity and cementation exponent for the same samples were measured and tabulated in Table 2.

Figure 2 shows the formation resistivity factor versus porosity measured at ambient conditions. In the measured cores a well defined relationship exists between formation resistivity factor and porosity. The formation resistivity factor was best fit to Archie's equation so that the coefficient (a) and cementation factor were determined. The data was fit to Archie equation by assuming $a=1$, and the value of m was calculated for each sample. The average cementation factor for all the core samples of Nubian sandstone was calculated from slope of the best fit straight line through the points. The average value of cementation factor was 1.69 and the correlation coefficient, R^2 , was 0.99.

$$\begin{aligned} \text{F.F} &= \phi^{1.69} \\ R^2 &= 0.99 \end{aligned}$$

Table 2. Porosity, formation factor, and cementation exponent for the samples at ambient conditions.

Sample #	Porosity (%)	Formation resistivity factor (F.F)	Cementation exponent "m"
03	10.39	41.6	1.65
10	9.01	52.8	1.65
15	12.17	44.6	1.80
18	14.59	23.9	1.65
24	8.01	60.4	1.62
29	17.38	20.3	1.72
41	15.34	23.3	1.68
42	11.71	41.8	1.74
47	17.91	20.0	1.74
53	11.16	36.8	1.64
83	9.56	59.0	1.74
123	12.76	33.5	1.71

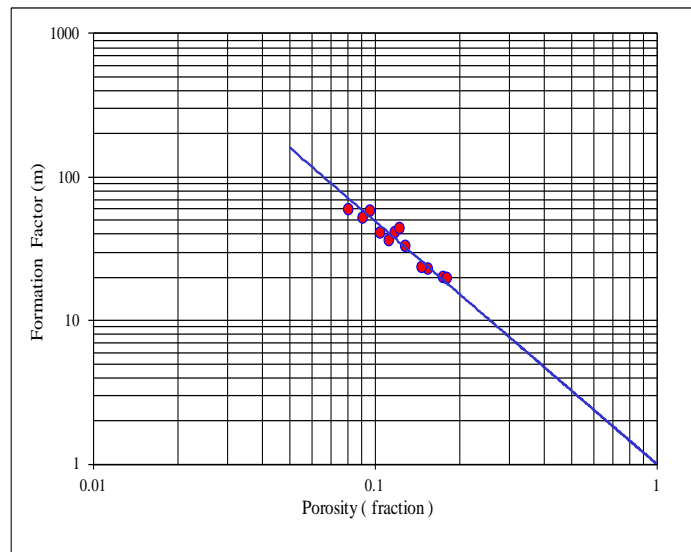


Fig 2. Porosity versus formation resistivity factor at room conditions.

In this study, both formation resistivity factor (FF) and cementation factor (m) were found increasing with confining pressure for the Nubian sandstone samples. Table 3 and Figure 3 display the experimental results that show the

effect of overburden pressure on cementation factor. Table 4 shows the individual results for porosity, formation resistivity factor and cementation exponent at different overburden pressures for sample # 03. Table 5 shows the results of saturation exponent (n) before and after wettability measurement.

Table 3. Cementation factor values at overburden pressure for selected samples.

Overburden pressure Psi	Cementation exponent (m)
1000	1.71
2000	1.72
3000	1.74
4000	1.75
5000	1.76

Table 4. Porosity, formation factor and cementation exponent for sample # 03 at different values of overburden pressure.

Pressure (Psi)	Porosity (%)	Formation factor (F.F)	Cementation exponent (m)
0	10.39	41.6	1.65
1000	10.11	44.6	1.66
2000	9.92	47.09	1.67
3000	9.82	49.21	1.68
4000	9.73	52.02	1.70
5000	9.68	54.52	1.71

Table 5. Saturation exponent values before and after wettability measurement

Sample #	Well name	(n) Before wettability measurement	(n) After wettability measurement
03	A1-Libya	1.39	2.39
10	A1-Libya	1.75	2.60
15	A3-Libya	2.06	2.79
18	B1-Libya	1.76	2.65
24	A3-Libya	1.93	2.18
29	C2-Libya	1.79	2.59
41	C1-Libya	1.87	2.50
42	A3-Libya	2.18	2.86
47	C2-Libya	1.91	2.65
53	A1-Libya	1.78	2.43
83	A2-Libya	1.97	2.49
123	A2-Libya	1.73	2.22

Figure 4 shows the relation between resistivity index and water saturation before and after wettability measurements for sample # 03. Drainage and imbibition capillary pressure curves for the sample were obtained and shown in Figure 5. The desired pressure is introduced into the apparatus, which allows the mercury to enter the rock sample. The pressure is introduced at a series of increasing pressure increments. The magnitude of pressure and the incremental volume of mercury injected into the sample are monitored and recorded after equilibrium.

Pore throat radius can be determined from mercury injection tests and may be used to categorize the rock by pore type as shown in Figure 6: macro, meso, and micro. Micro-porosity in reservoir rocks has been described as the pore system whose average pore diameter is less than 0.0625mm, Pittman (1971). Micro-pores can be in communication with larger pores or can be isolated and separate from the macro-porosity. Porosity logs see micro-porosity as part of the total porosity, but resistivity logs are affected to a large extent by the water contained in a micro-porous system. If micro-porosity is abundant enough and contains high immobile water, calculation of water saturation using conventional methods will erroneously yield high water saturation and the interval analyzed can be regarded as a water-bearing zone. Figure 7 shows the resistivity index versus water saturation and mercury saturation capillary pressure curves of sandstone for sample # 03. Good relation between resistivity and pore type system was observed. Note that the saturation where mercury penetration into micro-porosity occurs, a significant change in slope of the relationship between resistivity index and brine saturation of rocks also containing micro-porosity.

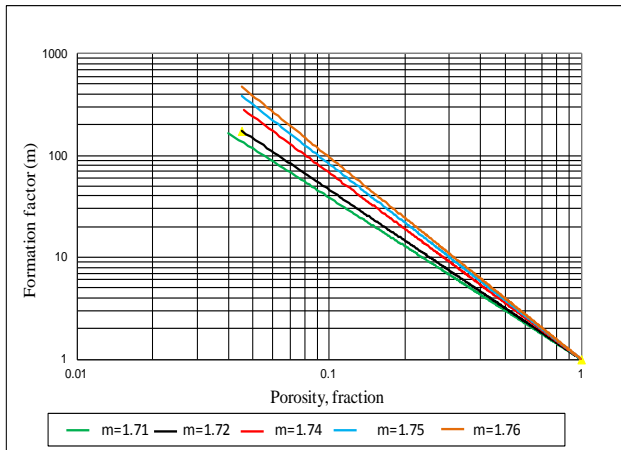


Fig. 3 Porosity versus formation resistivity factor at different values of overburden pressure.

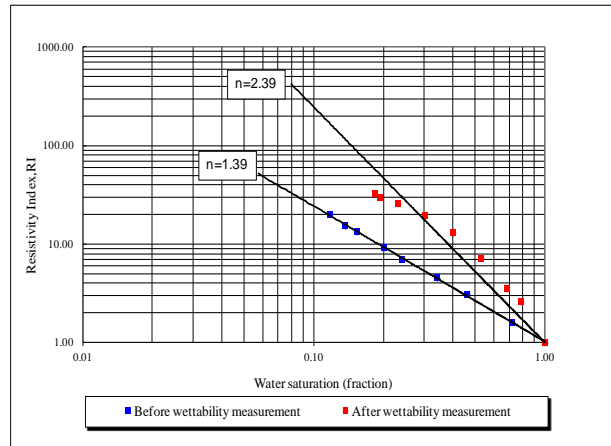


Fig. 4 Resistivity index versus water saturation before and after wettability test of sample # 03.

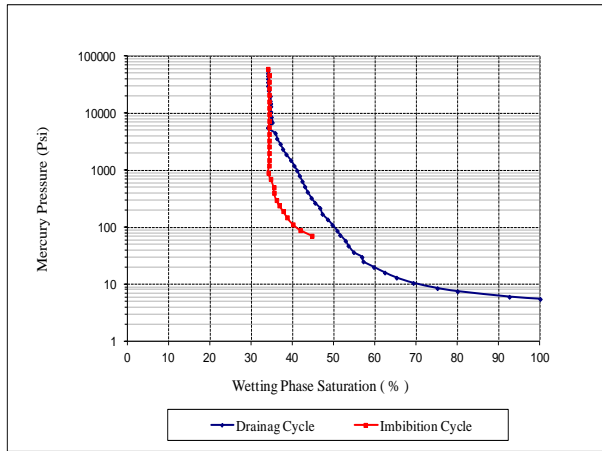


Fig.5 Drainage and imbibition cycles for sample # 03

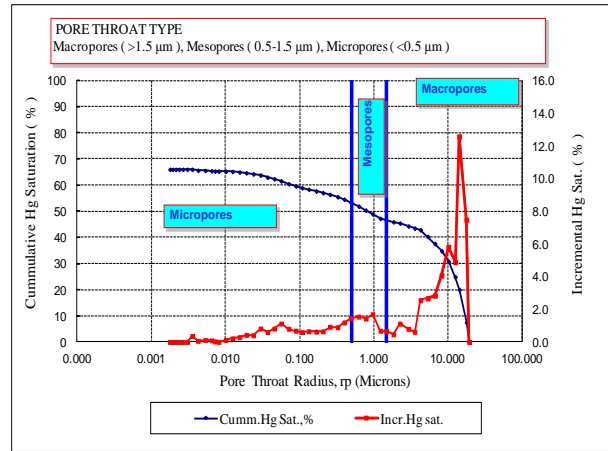


Fig. 6 Pore size distribution for sample # 03.

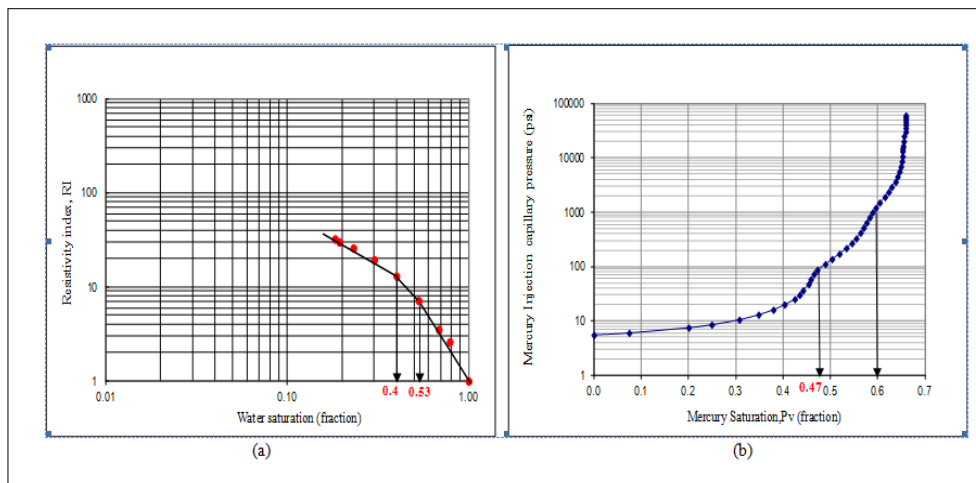


Fig. 7 Resistivity index versus water saturation and mercury capillary pressure versus mercury saturation for sample # 03.

Discussion

The Archie's cementation factor (m) was found to vary from 1.3 to approximately 2.2 for unconsolidated and consolidated sands respectively, Amyx (1962). Most previous studies showed that the formation resistivity factor and cementation exponent increase with overburden pressure. In this work, both formation resistivity factor (FF) and cementation exponent (m) were found to increase with confining pressure for the Nubian sandstone samples, Table 3.

In performing laboratory measurements, changes were observed in the resistivity of fluid filled reservoir rocks as a result of changing overburden pressure conditions. These changes may result from changing the internal pore structure and an increase in tortuosity and decrease in the effective cross-sectional area that is available for the flow of electric current. Table 3 and Figure 3 clearly show the relation. Table 4 summarizes the experimental results of the effect of overburden pressure and cementation exponent for sample # 03. A systematic decrease in rock conductivity and increase in formation factor as the overburden pressure increased over the range of 1000 to 5000 psi was seen. The overburden pressure was started at 1000 psi because during lab measurements the reduction effect of pore volume starts at pressure greater than 800 psi and ends at 5000 psi because the reservoir pressure is 5500 psi. The cementation exponent of sample # 03 was increased from 1.66 to 1.71 (+3.0%) as a result of increasing the pressure up to 5000 psi. Wyble (1958) showed that the cementation exponent (m) of one of the samples studied was increased from 1.87 to 2.04 (+9.1%) as a result of increasing the pressure up to 5000 psi. For sample # 03 the original value of porosity was 10.39% at zero overburden pressure, and formation factor 41.6. When the initial overburden pressure was applied (1000 psi) to the sample, the porosity decreased to 10.11% and the formation factor became 44.6. As the pressure was increased up to 5000 psi, porosity decreased to 9.68% and formation factor increased to 54.52. Thus, overburden pressure reduces the bulk volume. At low overburden pressures, fissures start to close with small compression in mineral grains. As the overburden pressure increases, the rock undergoes bulk compression resulting from pore and grain deformation. As the pressure is depleted in a reservoir, the effective overburden pressure increases causing a reduction in pore volume. The results indicate the rock is compacted as a result of overburden pressure, the matrix is under stress and porosity decreases, and therefore the cementation exponent would change.

The wettability of a system can range from strongly water-wet to strongly oil-wet. When the rock has no strong preference for either oil or water, the system is said to be of neutral (or intermediate) wettability. The wettability of hydrocarbon bearing rocks can be altered from its original water-wet state to oil-wet by adsorption of polar compounds or by adsorption of organic materials originally in the crude oil. This fact is true, in our results, for sample # 03 the saturation exponent before wettability measurement was 1.39, and when wettability test was conducted the sample imbibed oil (tendency to be oil wet), and the saturation exponent increased to 2.39. In water-wet rock, the brine occupies the small pores and forms a continuous film on the rock surface. In an oil-wet rock, the brine is located in the centers of the large pores. This difference in brine distribution caused by the wettability becomes very important as the brine saturation is lowered. Generally, almost all of the brine in the water-wet rock remains continuous, so the resistivity increases because of the decrease in cross-sectional area that can conduct flow. In oil-wet rock, a portion of the brine will lose electrical continuity, so the saturation exponent will increase at a faster rate. In oil-wet rock, a fraction of the non-wetting phase (specially at low brine saturation) which is located in the middle becomes disconnected and surrounded by oil which acts as an insulator to the flow of electric current. The insulation of this portion of brine prevents it from contributing to the flow of electric current and hence leads to higher values of saturation exponent.

The mercury injection method entails injecting mercury into a clean, dry sample and monitoring the injection pressure and the amount of mercury injected into the rock sample. Drainage and imbibition capillary pressure curves can be obtained. Modern mercury injection capillary pressure apparatus enables injecting mercury into a rock sample at high pressure. An injection pressure of up to 60,000 psi can be achieved. At this high pressure, pores down to 0.003 microns in diameter can be penetrated, which will yield a detailed pore size distribution.

The Amott wettability test was performed on plug samples from Nubian sandstone formation before porous plate capillary pressure test was conducted. By integrating of mercury injection capillary pressure curves and porous plate capillary pressure technique, the types of pore system were classified.

Initially, the mercury starts with low pressure injection until the macro-pores was saturated. The inflection point from this region was observed at about 100 psi, and the mercury saturation was 0.47 as shown in Figure 7 b. From porous plate capillary pressure test, the macropores region was observed during air injection at constant slope (n) until the sample reaches 0.53 water saturation as shown in Figure 7 a. The slope starts to change at 4 psi, at this point oil starts displacing water from large pores and the inflection point in the mercury injection capillary pressure curve was observed.

The mercury injection capillary pressure increases and the mercury starts to enter small pores (meso-pores). A second inflection point was seen at pressure about 1000 psi, and the mercury saturation was 0.6. The pressure continues to increase until the mercury fills the micro-pores as shown in Figure 7 b. In Figure 7 a, the slope (n) decreases toward lower water saturation as the pressure increases from 4 to 8 psi until the meso-pores were saturated at water saturation of 0.4.

A comparison was made between the mercury injection capillary pressure curve and resistivity index versus water saturation relationship, this indicates the second inflection point where the meso-pores was saturated. The remaining pores in the sample represent the micro-porosity at constant slope (n) and the relative volume of these micro-pores is a major factor controlling water saturation in oil and gas reservoirs. Thus, a good relationship between the type of pore system and resistivity was obtained in order to classify rock porosity type. Petrophysical characteristics such as porosity, recovery efficiency, irreducible water saturation, pore-throat size distribution and threshold capillary pressure are determined using mercury porosimeter. These characteristics determine the shape, slopes and plateau of the capillary-pressure curve. Analysis of the MICP curve is, therefore, important for various phases of reservoir production, especially secondary and tertiary recovery. These data may be evaluated in conjunction with additional SCAL and routine core petrophysical data in order to provide an accurate assessment of reservoir and/or seal potential.

The relationship between resistivity index and brine saturation of rocks containing micro-porosity is not linear, but the slope decreases towards the lower water saturation end. The reason is that, as oil saturation increases, first the larger pores dominate the resistivity. At this stage, water saturation is still high because micro-pores hold up a large water volume, which causes a high saturation exponent. As the oil starts to drain water from micro-pores, water saturation decreases sharply with little influence on resistivity and causes saturation exponent (n) to decrease with decreasing water saturation, Swanson (1985). The change in slope may be due to micro-pores/irregular surfaces through these samples.

Conclusions

The results show that changes were observed in formation resistivity factor and cementation exponent when overburden pressure was applied (slightly increases in cementation exponent with increasing O.B.P). Changes were also observed in the saturation exponent (n) and water saturation (S_w) before and after wettability measurements. Samples with an oil-wet tendency have higher irreducible brine saturation and higher Archie saturation exponent values than samples with a uniform water-wet surface. Mercury injection capillary pressure and resistivity index measurements demonstrated a good relationship between resistivity and type of pores (macro- and micro-pore system). As oil begins to penetrate micro-pore systems while measuring resistivity index versus brine saturation, a significant change in slope of the curve occurs.

Nomenclature

a	=	A constant in Archie's
A	=	Cross-Sectional area, cm ²
FF	=	Formation resistivity factor.
Kg	=	Gas Permeability, mD
L	=	Length, cm
m	=	Cementation factor,
n	=	Archie,s saturation exponent.
P1	=	Upstream Pressure,atm
P2	=	Downstream Pressure,atm

Pa	=	Atmospheric pressure, atm
Pc	=	Capillary pressure, psia
ΔP	=	Pressure differential, atm
Q	=	Volumetric flow rate, cc/sec
r_p	=	Pore throat radius, μm
R_w	=	Water resistivity, $\Omega\cdot\text{m}$
R_t	=	True resistivity, $\Omega\cdot\text{m}$
R_o	=	Rock resistivity, $\Omega\cdot\text{m}$
RI	=	Resistivity index
S_w	=	Water saturation, fraction
V_p	=	Pore volume, cc
V_b	=	Bulk volume, cc
V_g	=	Grain volume, cc
\emptyset	=	Fractional porosity
θ	=	Contact angle, degree
μ	=	Fluid viscosity, cp
σ	=	Interfacial tension, dyne/cm

Acknowledgment

We would like to take this opportunity to thank the people that have helped us to this work. The author acknowledges very much to Prof. David Potter, who patiently supervised the evolution of our work. He provided us with the invaluable academic advice, excellent guidance, endless assistance, moral support and critical review that led to the completion of our work. We wish also to express our sincere thanks to Libyan Petroleum Institute for providing the necessary data.

References

- Amyx, W. A., Daniel M. B., and Robert, L. W., 1960: "Petroleum Reservoir Engineering" McGraw-Hill Book Company, ISBN: 07-001600-3, p.610.
- Archie, G.E., "The electrical resistivity log as an aid in determining some reservoir characteristics", Trans. AIME, 1942 vol.146, pp.54-62.
- Keller G. V., 1953, "Effect of wettability on Electrical resistivity of sand" Oil and Gas Journal, January, pp.62-65
- Pittman, E. D., 1971, "Microporosity in Carbonate Rocks" AAPG Bull., Vol. 55, No.10 (October,1971), pp.1873-1881.
- Swanson, B. F., 1985, "Microporosity in Reservoir Rocks: Its measurements and influence on Electrical Resistivity" Trans. SPWLA, 26th Annual. Logging. Sympson, June 17-20.
- Washburn, E.W: "Note on a method of determining the distribution of pore size in a porous material" Proceedings of the National Academy of Science, 1921 v. 7, p.115-116.
- Wyble, D. O., "Effect of Applied pressure on the Conductivity, porosity, and Permeability of sandstones" Trans. AIME, 1958, Vol. 213, pp. 430-432

Biography

Hassan Sbiga is received his B.SC in petroleum engineering from Tripoli University - Libya in spring1992; and Master degree in petroleum engineering from Heriot-Watt University, Edinburgh-UK in 2005; and Doctor of Philosophy (PhD) in Petroleum Engineering from Heriot Watt University, Edinburg UK in 2013. Mr. Sbiga has 19 years experience in oil field and he is a member of SPE. His experience covered Routine and special core analysis, and participated in several joint venture studies concerning Libyan oil Reservoirs. He joined recently to reservoir

simulation studies section at LPI, and worked a Lecturer as a co-operator in different Universities and institutes in Libya giving Reservoir Rock Properties Course, Introduction to petroleum engineering, and others. He was selected by HWU as a staff to teach Formation Evaluation course in HWU School Branch in Libya in 2008. Mr. Sbiga also participated, presented, and published papers in national and international conference and journals in petroleum industry.

Saber Kh. Elmabrouk received the Ph.D. degree in Petroleum Engineering from the prestigious University of Regina, Canada. Prior to his Ph.D. he had earned his Master and Bachelor degree in Petroleum Engineering from University of Tripoli, Libya. Dr. Saber is currently assistant professor at University of Tripoli, Petroleum Engineering Department, Tripoli, Libya. Also, he is adjunct faculty at The Libyan Academy, Engineering Project Management Department, School of Applied Science and Engineering, Tripoli, Libya. His teaching and research career spans over 20 years. His research interests include reservoir management, well testing, phase behaviour, artificial intelligence techniques, modeling, optimization, and uncertainty and risk management

Walid Mohamed Mahmud received his B.Sc. degree in Petroleum Engineering from the University of Tripoli, Libya in 1995, M.E. and Ph.D. degrees in Petroleum Engineering from the University of New South Wales, Sydney, Australia in 1997 and 2004, respectively and an MBA from the University of Southern Queensland, Toowoomba, Australia in 2007. He is currently an Assistant Professor at the University of Tripoli, Libya. He has industry experience as a Business Development Manager and Senior Reservoir Engineer at Heinemann Oil GmbH in Austria and Libya. Dr. Mahmud is also an assistant professor at the Department of Petroleum Engineering, the University of Tripoli. His main general teaching and research interests are fluid flow in porous media, network modeling, two and three-phase relative permeability and reservoir characterization and management. His current research interests include two and three-phase flow, two and three phase relative permeability, numerical network models and formation evaluation.